Proc. SPIE, Vol. 4277, 144 (2001), Photonics West 2001, paper 4277-18 (invited)

Nonlinear Integrated Optical Frequency Converters with Periodically Poled Ti:$LiNbO_3$ Waveguides

G. Schreiber, D. Hofmann, W. Grundkötter, Y. L. Lee, H. Suche, V. Quiring, R. Ricken, and W. Sohler

Universität Paderborn, Angewandte Physik, Warburger Str. 100, D-33098 Paderborn, Germany

ABSTRACT

The development of a whole family of near and mid-infrared quasi-phase matched parametric frequency converters with periodically poled in Ti:(Er:)$LiNbO_3$ waveguides is reviewed. Due to high quality waveguides with very low losses and excellent homogeneity unprecedented conversion efficiencies have been achieved for second-harmonic generation, difference-frequency generation, optical parametric fluorescence and doubly as well as singly resonant optical parametric oscillation.

Keywords: nonlinear optics, parametric frequency conversion, lithium niobate, quasi-phase matching, second-harmonic generation, difference-frequency generation, optical parametric fluorescence, optical parametric oscillation

1. INTRODUCTION

The advent of the electric field poling method to fabricate periodically poled $LiNbO_3$ resulted in a renaissance of nonlinear optics. Since then quasi-phase matching has been used for wavelength conversion in devices like frequency doublers, difference frequency generators and optical parametric oscillators. In the past primarily bulk devices have been used because of the ease to fabricate periodically poled bulk materials. A significant improvement in device efficiency in comparison to bulk frequency converters is expected by employing the integrated optics approach. Therefore, nonlinear waveguides based on periodically poled materials like $LiNbO_3$ are attracting considerable interest as frequency converters of (tunable) laser radiation with high conversion efficiency and spectral resolution for applications in telecommunication and life sciences. Recent advances of microfabrication technology enable the fabrication of very long, homogeneous, periodically poled Titanium-diffused waveguides in $LiNbO_3$ of very low losses. These waveguides enabled the development of a whole family of quasi-phase matched $\chi^{(2)}$ devices which will be presented in the following.

In the 2nd chapter we describe our fabrication technology to obtain very long, homogeneous, periodically poled Ti:(Er:)$LiNbO_3$ waveguides of low losses in the near- (NIR, 1 μm$< \lambda <$ 2 μm) and mid (MIR, 2μm$< \lambda <$ 5μm)-infrared spectral range. Second harmonic generation (SHG) and self-frequency doubling with NIR waveguides is reported in the 3rd chapter. Difference frequency generation (DFG) for both the NIR- and MIR-range will be presented in chapter 4. The combination of very efficient second harmonic generation and simultaneous difference-frequency generation led to the development of cascaded-difference frequency generators (cDFG) with more than 100 % efficiency and simultaneous parametric amplification. Stimulated optical parametric fluoresence (OPF) has been used to generate nonresonant tunable radiation (chapter 5). Doubly resonant integrated optical parametric oscillators (DR-IOPO) with oscillation thresholds of about 10 mW and several hundred nanometer tuning range have been demonstrated with NIR- and MIR-IOPOs (chapter 6). Finally, we report about the first room temperature continuous wave MIR singly resonant IOPO with a threshold significantly below 1 W and large tuning range (also chapter 6).

Further author information: (Send correspondence to G. Schreiber)
G. Schreiber: E-mail: G.Schreiber@Physik.Uni-Paderborn.de

2. WAVEGUIDE FABRICATION AND CHARACTERISATION

Fabrication Fig. 1 of the nonlinear integrated optical frequency converters starts with the optional indiffusion of a 25-30 nm thick erbium layer into the -Z face of a 0.5 mm thick and up to 100 mm long Z-cut $LiNbO_3$ sample. Due to the small diffusion constants of erbium into $LiNbO_3$ we diffuse at 1130°C for 150 h. Erbium diffusion is attractive because this allows to combine quasi-phase matched nonlinear frequency conversion in an amplifying or even laser active medium. Afterwards, a waveguide is fabricated by indiffusion of a photolithographically defined Ti-stripe. For waveguides, single mode in the near infrared, the Ti-stripes are 7 μm wide and 98 nm thick. Indiffusion is performed at 1060°C over 7.5 h in an argon inert gas atmosphere and a subsequent 1 h postdiffusion is done at the same temperature in oxygen to reoxidize the material. To fabricate nonlinear waveguides, singe mode in the mid-infrared,

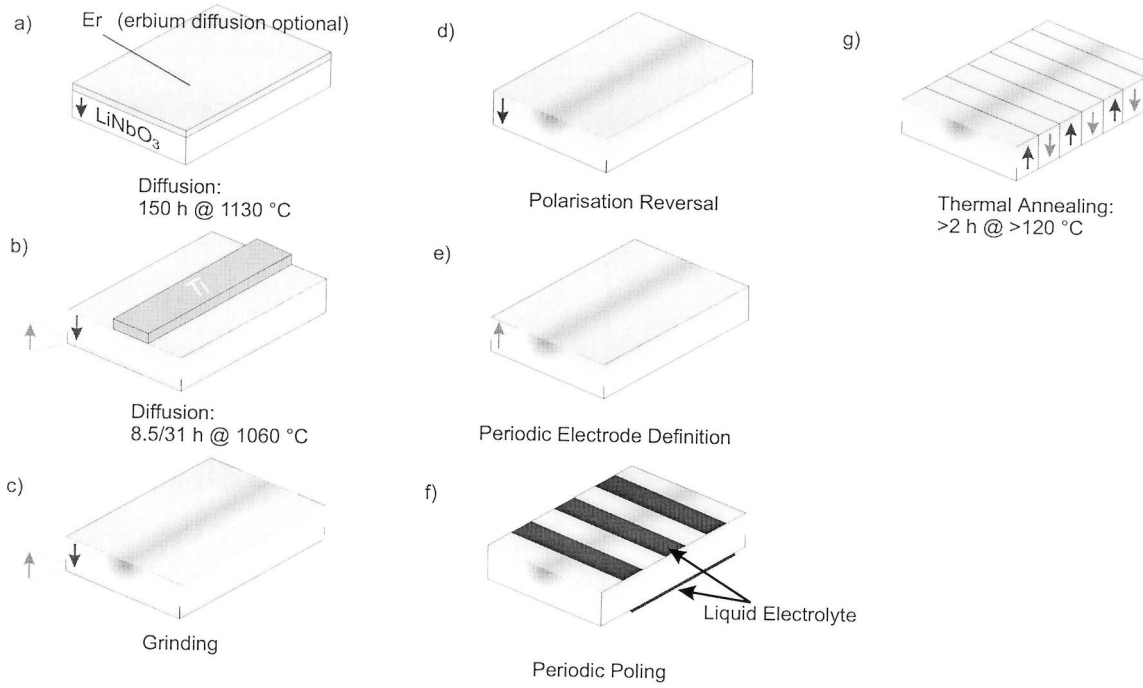

Figure 1. Fabrication of periodically poled Ti:$LiNbO_3$ waveguides (Erbium-doping optional): a) evaporation of an erbium layer onto the -Z face and subsequent indiffusion; b) photolithographic definition of a Ti-stripe and indiffusion afterwards; c) removal of a domain inverted layer on the +Z face; d) reversal of the spontaneous polarization of the sample as a whole; f) definition of the periodic electrode; f) electric field poling; g) thermal annealing.

we indiffuse 20 μm wide and 160 nm thick Ti-stripes into the -Z face at the same temperature for 31 h. We found that a subsequent electric field poling is not possible after Er and/or Ti-indiffusion due to a shallow domain inverted layer on the +Z side of the sample. To obtain a single domain sample again we have to remove this layer by careful grinding. In order to get a periodic microdomain structure with an excellent homogeneity a two step electric field poling technology has been developed. With the first field poling process we reverse the spontaneous polarization of the complete substrate. In this way the waveguides come to the preferred +Z-face for periodic poling. As the microdomains start their growth always from the +Z-face we realize the periodic electrode on that side. A periodic photoresist structure ($\sim$ 17 μm for NIR-waveguides and $\sim$ 31 μm for MIR-waveguides) and LiCL in isopropylalcohol as electrolyte is used to form the electrode. Periodic poling is then accomplished by application of high voltage to exceed the coercitive field strength of $LiNbO_3$ of about 21 kV/mm. We control the poling process by monitoring the current flow through the crystal. Poling is stopped, when the charge Q corresponds to an empirically determined value to get a 50 % duty cycle of the domain pattern. The total length of the periodically poled region is up

to 90 mm. Finally, thermal annealing at >120°C over >2 h is performed to reduce the optical losses induced by electrical and mechanical stress. After polishing of the endfaces we characterize our samples by several means. To reveal the domain pattern quality selective etching of the sample surface by a concentrated $HF:HNO_3$ acid can be done. Fig. 2 shows several photographs of different selectively etched samples. We did not observe any differences with respect to the process of periodic poling and to the quality of the domain pattern between doped and undoped samples. A near infrared sensitive camera can be used to confirm that the waveguides are single mode in the spectral region of interest. Typically, the losses in extraordinary polarization range from 0.1...0.2 dB/cm in the NIR- and 0.03...0.06 dB/cm in the MIR-spectral region. A confocal second-harmonic generation microscope can be used to visualize the microdomain grating in vertical and lateral direction with high resolution (Fig. 3).[1]

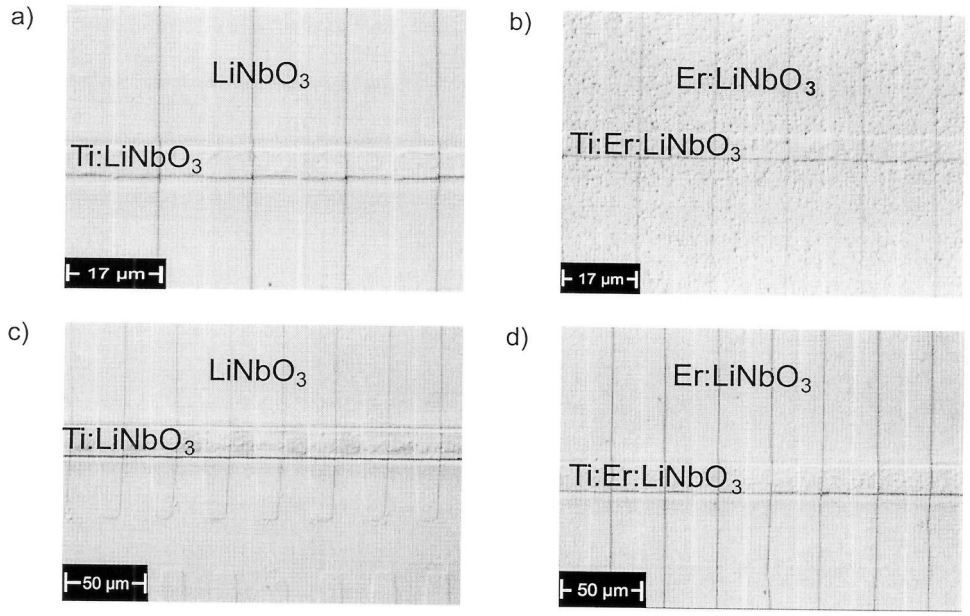

Figure 2. Photographs of selectively etched surfaces a) $Ti:LiNbO_3$ waveguide with a 17 μm grating; b) dto. with erbium; c) $Ti:LiNbO_3$ waveguide with a 31 μm grating; b) dto. with erbium.

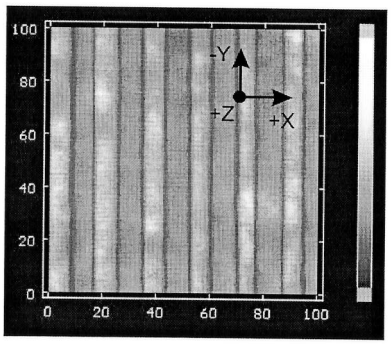

Figure 3. Photograph of a periodically poled sample taken with a confocal SHG microscope.

3. SECOND HARMONIC GENERATORS

3.1. NIR Frequency Doubler

The nonlinear performance of a periodically poled waveguide is characterized by measuring the phase-match characteristics of second-harmonic generation and the normalized efficiencies. As light source of fundamental wavelength we use a fiber coupled tunable (1500 nm $< \lambda_f <$ 1580 nm) external cavity semiconductor laser. Its radiation is polarization controlled and launched into the waveguide by butt-coupling. With 1.16 mW coupled fundamental power we achieved a maximum of 12.6 μW of generated second-harmonic power. This corresponds to a normalized efficiency of 935 %W^{-1}. The phase matching curve has only slight deviations from the ideal sinc^2 form with a full width at half maximum of $\sim$ 0.15 nm (see Fig. 4). This result demonstrates the very good homogeneity of the waveguide and of the microdomain pattern.

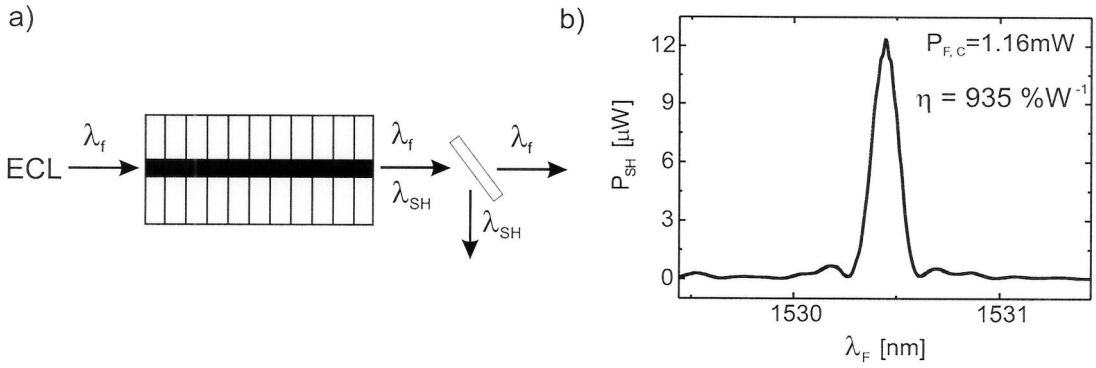

Figure 4. a) Schematical setup for SHG and b) measured SH phase-match curve.

3.2. Self-Frequency Doubling Laser

Since the first demonstration of an Er-diffusion-doped $LiNbO_3$ waveguide laser more and more advanced laser designs have been implemented taking advantage of the excellent electro- and acousto-optical properties of $LiNbO_3$.[2] On the other hand, periodic poling of ferroelectric Ti:$LiNbO_3$ waveguides led to the development of quasi-phase-matched nonlinear frequency doublers of unprecedented efficiency. Therefore, the combination of quasi-phase-matched frequency conversion in amplifying or even laser active waveguides would allow to develop a whole new class of integrated optical devices. In the following we describe the realization of a self-frequency doubling Ti:Er:$LiNbO_3$ waveguide laser.

A fiber-optic wavelength division multiplexer was used to couple up to 135 mW of pump radiation of a high power semiconductor laser diode at 1480 nm center wavelength into the Ti:Er:$LiNbO_3$ waveguide resonator (see Fig. 5). The input mirror was a tunable, low finesse Farby-Perot etalon, formed by the end face of the optical fiber and the polished, uncoated front face of the waveguide. The fiber was mounted on a piezo-driven translator allowing to adjust thickness of the air gap and in this way the effective (wavelength dependent) reflectivity of the etalon between 5 % and 30 % ("tunable air gap reflector"). Due to its wavelength dependence the preferred laser wavelength could be selected among emission at λ_L = 1531 nm, 1546 nm, 1575 nm and 1602 nm. The output mirror was a dielectric multilayer (12 layers) vacuum-deposited on the polished rear waveguide end face with a broadband reflectivity of $>$ 95 % in the wavelength range 1480 nm $< \lambda <$ 1800 nm. Around 765 nm the mirror transmission was high, exceeding 80 %.

To render quasi-phase-matched SHG possible in the periodically poled ($\Lambda = 17\mu$m) waveguide at room temperature the emission wavelength λ_L = 1531 nm was adjusted. In this configuration the laser threshold was at 87 mW coupled pump power. Due to waveguide losses the slope efficiency was poor allowing only up to 2.4 mW of output power. Simultaneously, frequency doubled radiation λ_{SH} = 765.5 nm was generated and emitted in both, forward and backward directions. Only the part, emitted in forward direction, was measured using an optical spectrum analyzer as a wavelength filter to suppress the green upconversion light generated in the Er-doped waveguide. Up to 2.7 μW of SH-power was emitted with a quadratic dependence on the fundamental laser power (see Fig. 5). Photorefraction

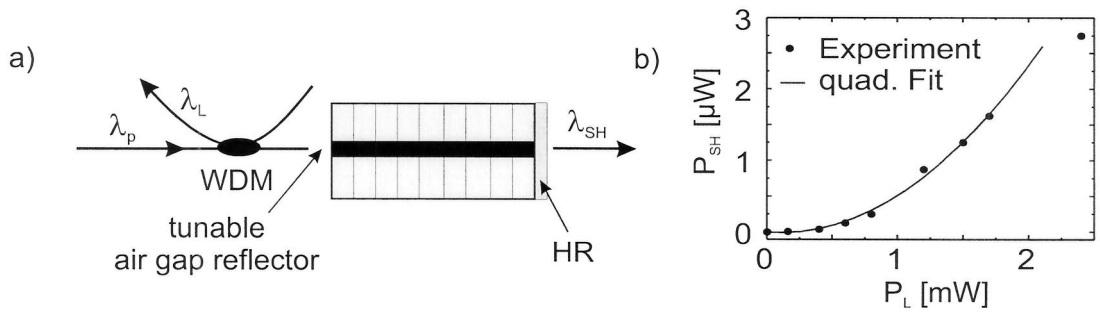

Figure 5. a) Schematical setup for investigation of self-frequency doubling of a periodically poled Ti:Er:$LiNbO_3$ laser.
b) Measured second harmonic power as function of the laser output.

effects induced some instabilities, which are currently investigated in more detail. To improve the performance of the laser we used a narrow bandwidth fiber Bragg grating as mirror of high reflectivity instead of the dielectric end face mirror and the "air gap reflector" (see Fig. 6). This fixed the fundamental laser wavelength and increased the intracavity field strength leading to an enhanced SH-conversion efficiency ($P_{SH} \sim 20\ \mu W$ in both configurations).

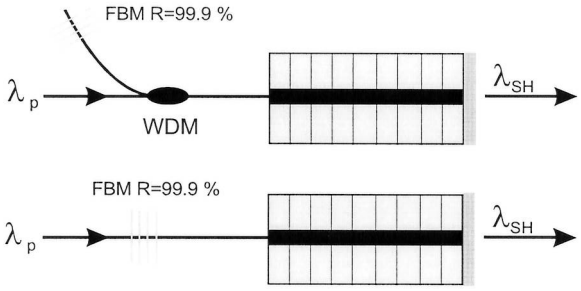

Figure 6. Self-frequency doubling waveguide lasers with fiber-bragg gratings as input mirrors.

4. DIFFERENCE-FREQUENCY GENERATORS

Wavelength conversion in wavelength-division-multiplexed (WDM) and time-division-multiplexed (TDM) optical networks is a key technology of future high bit-rate transport systems. Wavelength conversion offers a higher flexibility in traffic management and a dynamic reconfiguration of the optical network. In recent years, difference-frequency converters based on periodically poled $LiNbO_3$ waveguides attracted considerable interest, because they fulfill numerous requirements for ideal wavelength converters for telecommunications such as strict transparency, independence of bit rate and data format and low cross talk.[3] They offer a high conversion efficiency without attenuation of the signal and adding only negligible noise from spontaneous fluorescence. In addition, the wavelength conversion bandwidth is high and it is possible to cascade many converters. The simultaneous conversion of many wavelength channels, spectral inversion and parametric amplification are also attractive properties of difference-frequency converters.
Many atmospheric trace gases like HF, H_2CO, CH_4, NO, N_2O, SO_2, and CO have their fundamental absorption bands in the mid-infrared (MIR) spectral range . Therefore, sensitive environmental sensing is possible using corresponding MIR (coherent) radiation. Existing lasers have different drawbacks such as limited tunability, low spectral resolution, high power consumption, large size, fragility, and some require (cryogenic) cooling. As a consequence new compact mid-infrared sources for room temperature operation are required. Tunable coherent emission in the MIR can be generated by difference-frequency generation (DFG) in nonlinear bulk crystals or nonlinear waveguides. In comparison with bulk configurations there is no trade-off in waveguides between mode size and interaction length.

Hence, in long structures the guided wave conversion efficiency considerably exceeds the efficiency of a bulk optics approach.
Because of the excellent homogeneity of periodically poled Ti:$LiNbO_3$ waveguides they should be ideal candidates for very efficient near- and mid-infrared difference frequency generators. In the following we report quasi-phase matched difference-frequency generation with up to 200 % resp. 105 $\%W^{-1}$ in the near- resp. mid-infrared spectral region.

4.1. NIR Difference-Frequency Generator

A cw Titan-Sapphire laser at 779.5 nm wavelength was used as pump laser in a DFG experiment. Photorefractive effects were avoided by performing the experiment at 90 °C. The signal laser was a fiber coupled external cavity semiconductor laser tunable from 1500 to 1580 nm. A special wavelength division multiplexer has been used to couple pump and signal beams into a single mode fiber of 780 nm second order mode cutoff; it was butt-coupled to the waveguide end face. In this way mainly the fundamental modes were excited (Higher order pump modes would lead to weak DFG at other wavelengths due to the altered phase-match condition). The coupling was mechanically optimized by observing the second-harmonic power generated by the tunable laser.

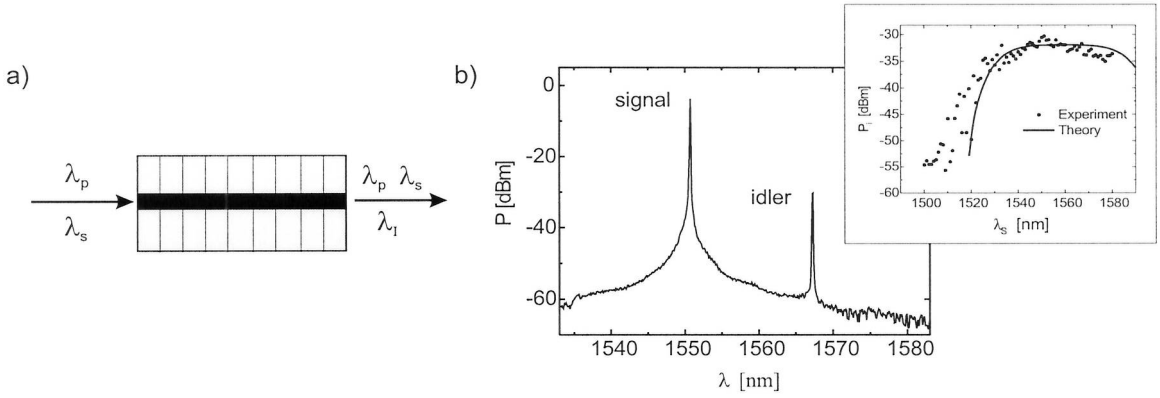

Figure 7. Schematical setup (left) and spectral characteristic of signal and idler (right). The inset shows the idler power as function of the signal wavelength.

We used 260 μW of coupled pump power and 1.1 mW of coupled signal power. Fig. 7 shows the optical output spectrum for a signal of 1551 nm wavelength, leading to an idler wave (at the difference frequency) at 1568 nm. The conversion efficiency was 318 % W^{-1} resp. 12.7 $\%W^{-1}cm^{-2}$; the generated idler power was 930 nW. We attribute the difference to the SHG efficiency mainly to a nonideal coupling efficiency to the fundamental mode of the waveguide. The DFG conversion bandwidth was measured by tuning the external cavity laser from 1500 nm to 1580 nm (inset at Fig. 7). The 3 dB bandwidth for this device was 55 ± 5 nm. This bandwidth agrees well with the 56 nm bandwidth predicted from theory.

4.2. NIR Cascaded Difference-Frequency Generator

The demonstration of second-harmonic generation (SHG) of unprecedented efficiency in PPLN waveguides opened the possibility to combine SHG and DFG in a single device or even in the same waveguide or structure[5,6] In such a cascaded-difference frequency generation (cDFG) device a strong fundamental wave at λ_f is used to generate a pump wave at $\lambda_p = \lambda_f/2$ by frequency doubling.[7] Simultaneously, the pump wave interacts with a signal wave at λ_s to generate an idler wave at $\lambda_i^{-1} = \lambda_p^{-1} - \lambda_s^{-1} = 2\lambda_f^{-1} - \lambda_s^{-1}$. In the following we report about cascaded difference frequency generation in continuous wave and pulsed mode operation.

Continuous wave cDFG

Fig. 8 (left) shows the setup to investigate cascaded difference frequency generation. The fundamental laser source for the frequency doubling process was a tunable semiconductor laser (external cavity laser: ECL2). As signal laser we used the second ECL1. The preamplified fundamental and (unamplified) signal radiations were superimposed in

a single fiber using a 50/50 fiberoptic coupler. By using a high power erbium doped fiber amplifier (HP-EDFA) we boosted the total incident power to 320 mW with a fundamental- to signal power ratio of 16 dB (P_f=213.7 mW; P_s=5.3 mW, ASE power=101 mW). Despite the preamplification of the fundamental source a significant amount of amplified spontaneous emission (ASE) was superimposed to the boosted fundamental- and signal radiation, as the HP-EDFA was not operated in saturation. To avoid photorefractive effects we operated the frequency converter at 200°C. The EDFA-amplification bandwidth limited the maximum temperature to 200°C as the resulting phase-matching wavelength for second-harmonic generation shifted to 1577 nm.

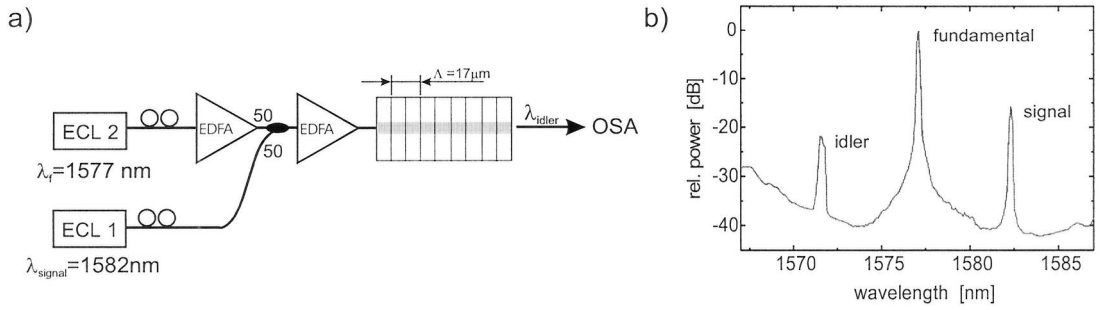

Figure 8. a) Schematical setup to investigate cDFG in continuous wave operation.
b) Spectral characteristic of fundamental, signal and idler waves.

In continuous wave operation of the wavelength converter we measured a ratio between the output levels of signal and idler of -6.1 dB (see Fig. 8 right). This corresponds to a conversion efficiency of 24.5 % and a power level of the converted signal of 1.3 mW Due to the operation at 200°C the signal and idler output power was very stable as function of time without any fluctuations induced by photorefractive effects. Due to the fairly long fundamental wavelength for phasematching at 200°C it was not possible to completely saturate the HP-EDFA leading to an increasing amount of ASE especially towards shorter wavelengths. Fig. 9 demonstrates the broadband tuning behaviour of a a cascaded difference frequency generator at low power levels at room temperature.

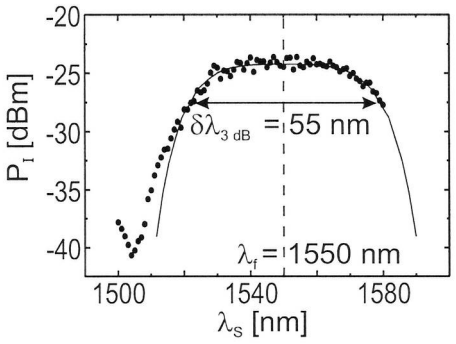

Figure 9. Generated idler power as function of the signal wavelength.

Pulsed cDFG

Fig. 10 shows the setup for cDFG in a pulsed mode. The fundamental source was a modelocked integrated optical Ti:Er:$LiNbO_3$ laser with a repetition rate of 1.8973 GHz (2nd harmonic modelocking) resp. 9.93 GHz (10th harmonic modelocking) and 1562nm center wavelength. Using an optical autocorrelator a pulse width of 12.4(6) ps was measured leading to a pulse duty cycle of -16(-12.3) dB. With an optical spectrum analyzer of 0.1 nm resolution a spectral width (FWHM) of 0.35(0.65) nm was determined. This leads to a time-bandwidth-product of 0.52(0.48), slightly exceeding the transform limit for gaussian pulses. The modelocked fundamental source was boosted to an

average power of 88 mW using the same high power EDFA as before. Phase-matching was achieved at a temperature of 100°C. The SHG-pulses are about a factor of $\sqrt{2}$ shorter thus leading to a duty cycle of -17.5(-13.8) dB for the 12.4(6) ps long fundamental pulses. An external cavity laser operated at 1557 nm was used as the signal source. Fundamental and signal radiation were combined with a 90/10 fiber optical coupler.

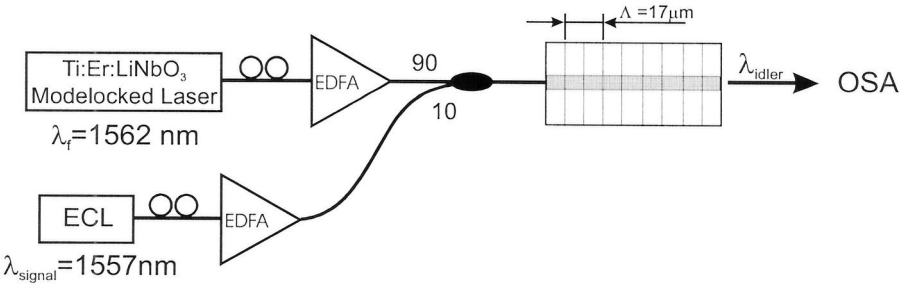

Figure 10. Experimental setup for cascaded DFG for pulsed mode operation.

Fig. 11 (left) shows the measured spectral characteristics of our frequency converter for pulsed pumping at 2 GHz (sample temperature 100°C). With an incident signal power of 2.8 dBm (cw) an average converted idler power 14.5 dB below the transmitted signal power has been measured. This leads together with the idler pulse duty cycle of -17.5 dB to a peak conversion efficiency of +3 dB and to simultaneous optical parametric amplification of the signal by +3 dB. The estimated peak power of the converted pulses is 1.9 mW assuming a coupling and transmission loss of the signal of 3 dB.
We also performed experiments at about 10 GHz repetition rate. Due to the broader fundamental spectrum of about 0.65 nm and some photorefractive damage due to the larger pump duty cycle (-12.3 dB) it was not possible to achieve a conversion efficiency >0 dB (see Fig. 11 right). On the other hand the measured efficiency of -4.6 dB is to our knowledge the best result reported to date at such a high repetition frequency.

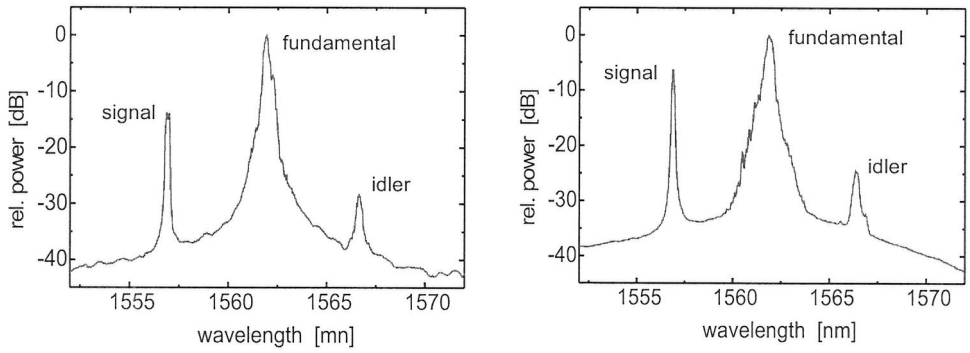

Figure 11. Optical output spectrum at 2 GHz (left) and 10 GHz (right).

NIR Amplified Cascaded Difference-Frequency Generator

Additional improvement of the performance of a cascaded difference frequency generator can be achieved by using periodically poled Ti:Er:$LiNbO_3$ waveguides. In this way it is possible to combine nonlinear frequency conversion and amplification of fundamental, signal and idler radiation in the same waveguide structure. Fig. 12 shows the setup to investigate amplified cascaded difference-frequency generation. We used a wavelength-division multiplexer (WDM) to couple the pump at 1480 nm into the waveguide. Without nonlinear conversion an amplification of +3 dB has been measured at a wavelength of 1576 nm. The coupled pump power was ~ 90 mW. With nonlinear conversion

we achieved amplification of the idler radiation at the same wavelength of up to 4.4 dB at $\sim$ 110 mW pump power. Fig. 13 illustrates the generated idler power as function of the coupled pump power.

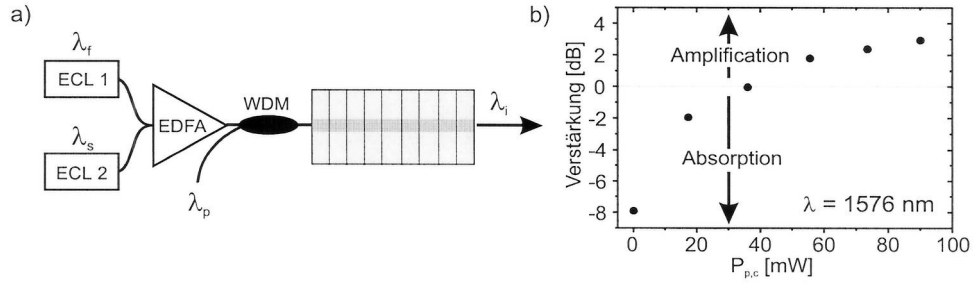

Figure 12. a) Experimental setup and b) amplification as function of the coupled pump power.

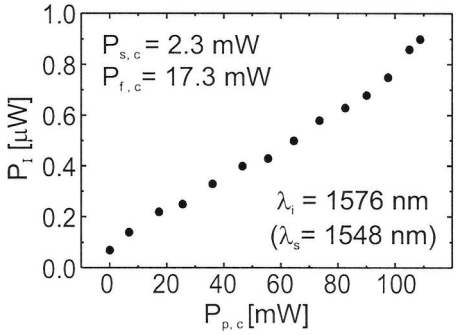

Figure 13. Generated idler as function of the coupled pump power.

4.3. MIR Difference-Frequency Generator

Fig. 14 shows the experimental set-up to perform MIR-DFG experiments.[8] We used a single-frequency fiber coupled external cavity semiconductor laser as pump laser tunable from 1500 to 1580 nm with a maximum output power of 2 mW. The pump radiation was amplified by an erbium doped fiber amplifier up to 11 mW in the 1520 to 1580 nm spectral range. The signal laser was a He-Ne laser with 1 mW output power at $\lambda = 3391$ nm. Superimposing of the two laser beams was done by using a dichroic beam splitter of high reflectivity around 3391 nm and high transmissivity around 1550 nm. The combined beams in TM polarization were focused in the Ti:$LiNbO_3$ waveguide by a CaF_2 lens. By a second lens of the same type the signal and the generated idler radiations were focused on a lead sulfide (PbS) or a lead selenide (PbSe) photoconductive detector. The pump radiation was absorbed by a Ge filter in front of the detector. The attenuation of the periodically poled waveguides has been investigated in TM-polarization at $\lambda =$ 3391 nm ; we measured losses in the range of 0.03 to 0.25 dBcm^{-1} with no significant difference between periodically and homogeneously poled waveguides. At this wavelength (signal wavelength of DFG) only the fundamental mode is guided. The phase matching curve in Fig. 14 (right) presents the generated idler power (measured with the PbS detector) as function of the pump wavelength at room temperature for both experiment and theory at constant signal wavelength ($\lambda_s = 3391$ nm); the investigated waveguide has a domain period of $\Lambda = 31.4$ μm and losses of 0.03 dBcm^{-1}. The maximum idler power measured with the PbSe detector at optimum phase matching was around 230 nW. With coupled power levels of 2 mW (pump) and 110 μW (signal) (measured also with the PbSe detector) a maximum conversion efficiency of 105 %W^{-1} has been achieved; this conversion is normalized to the pump power level. The halfwidth of the experimental characteristic of 2.8 nm is best reproduced by a modelled response if an effective interaction length of 68 mm is taken into account. This result demonstrates that 85 % of the 80 mm

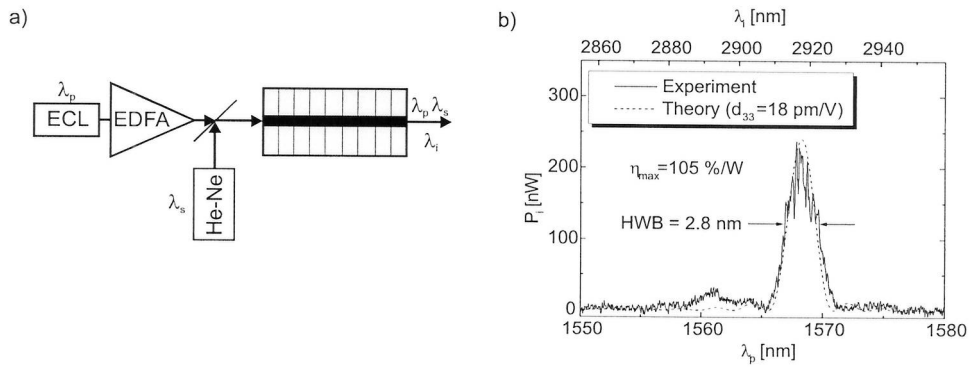

Figure 14. a) Experimental setup and b) phase-match curve of MIR-DFG.

long periodically poled waveguide contributed to the frequency conversion process; the waveguide homogeneity is excellent. Fig. 15 shows calculated phase matching tuning curves at fixed temperatures together with experimental values at fixed signal wavelength of a 30 μm wide and 50 mm long waveguide with a QPM period of 31.2 μm. More than 100 nm tuning of idler wavelength is accessible by only 40 K temperature change.

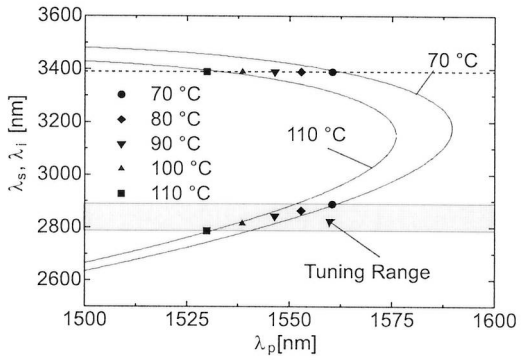

Figure 15. Temperature tuning characteristic of MIR-DFG.

5. OPTICAL PARAMETRIC FLUORESCENCE GENERATORS

Optical parametric fluorescence (OPF) describes the spontaneous decay of pump photons into signal- and idler-photons by the influence of the zero-point fluctuations of the electromagnetic vacuum field. This process, which is determined by energy-and wave vector-conservation, can be stimulated and exploited to generate tunable broadband radiation without the need of resonant structures. The spectral bandwidth of the emission strongly depends on parameters like pump wavelength, pump power and interaction length. Nonlinear waveguides are very attractive devices for the generation of stimulated OPF because of the high intensity of the pump wave and very long interaction lengths. We examined the nonresonant generation of tunable radiation for the near- and mid-infrared spectral region.

5.1. NIR Optical Parametric Fluorescence

A tunable Ti:Sapphire laser has been used as pump source in a NIR-OPF generator. The Fig. 16 (left) shows the experimental setup to investigate OPF. An optical spectrum analyzer has been used to measure the tuning and spectral characteristic of the OPF generator. The Fig. 17 shows the tuning behaviour at a coupled pump-power level of 10 mW. By tuning the pump wavelength from 766-776 nm we observed signal and idler emission from

1200-2000 nm. The insets in Fig. 17 show the spectral characteristic of the emission at selected pump wavelengths. Close to the wavelength of degeneracy broadband emission with a spectral width of $\sim$ 150 nm has been observed. As we moved away from degeneracy we obtained narrower emission. This behaviour is due to the more stringent phase-match condition. Increasing the pump power led to strong stimulated emission with exponential growth of the generated radiation (see Fig. 16 (right)) and to a narrowing of the linewidth of the emitted radiation .

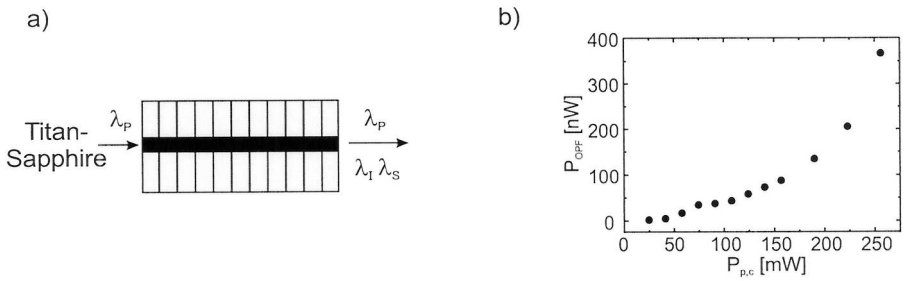

Figure 16. a) Experimental setup to investigate OPF in the NIR spectral range.
b) Power of the stimulated OPF-radiation as function of the coupled pump power.

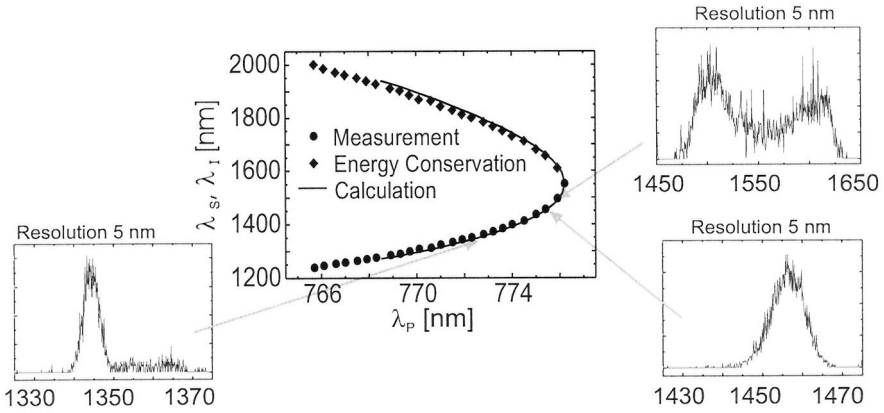

Figure 17. Tuning and spectral characteristic of NIR-OPF at selected wavelengths.

5.2. MIR Optical Parametric Fluorescence

For the investigation of OPF in the MIR an amplified tunable semiconductor laser has been used as pump source. The Fig. 18 (right) shows the tuning behaviour. Limited by the amplification bandwidth of our high-power erbium fiber amplifier, a tunable OPF emission from 2750-3480 nm could be generated. The maximum output power was 2.3 nW at an external pump power of 1.5 W.

6. OPTICAL PARAMETRIC OSCILLATORS

Integrated optical parametric oscillators (IOPOs) are attractive devices to generate tunable coherent radiation in a broad tuning range. Contrary to their bulk counterparts IOPOs promise a low oscillation threshold, low waveguide losses provided. The first near-infrared doubly resonant IOPO with a high finesse Ti:$LiNbO_3$ waveguide resonator was already demonstrated in 1981, using birefringent phase matching. An improved version had a threshold of only 26 mW incident pump.[9]
The advent of the quasi-phase-matching scheme in periodically poled $LiNbO_3$ should allow a threshold reduction of

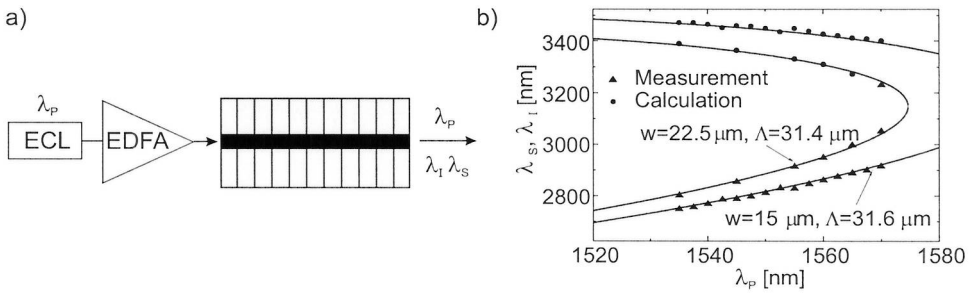

Figure 18. a) Setup and b) tuning characteristic of MIR-OPF.

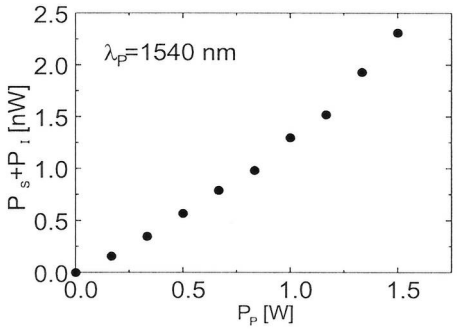

Figure 19. Power characteristic of the OPF as function of the pump power.

at least one order of magnitude due to the exploitation of the highest nonlinear coefficient in $LiNbO_3$. However, up to now near-infrared devices with proton exchanged waveguides had a threshold in the W-regime[10,11] Based on our periodically poled Ti:$LiNbO_3$ waveguides we developed doubly as well as singly resonant IOPO in the near- and mid-infrared spectral regions with unprecedented properties.

6.1. NIR Optical Parametric Oscillator

Using a periodic microdomain pattern with a period of ~17 μm over a total length of 80 mm we were able to realize the first cw doubly resonant near-infrared optical parametric oscillator with a periodically poled Ti:$LiNbO_3$ waveguide.[12] Typical waveguide losses were between 0.09 and 0.2 dB/cm. The endfaces of the samples were coated with dielectric mirrors with a high transmission for the pump (~ 780 nm, T>90 %) and a high reflectivity for the signal and idler waves around 1550 nm (R>95 %) (see Fig. 20). Oscillation started near degeneracy at a coupled pump power of 4.2 mW only. Fig. 21 shows the measured output power of signal and idler P_s+P_i as function of the coupled pump power $P_{p,c}$. The slope efficiency is ~3 %. Tuning of the IOPO was determined by the wavelength range of mirror reflectivity exceeding 87 % (Fig. 20 (right)).

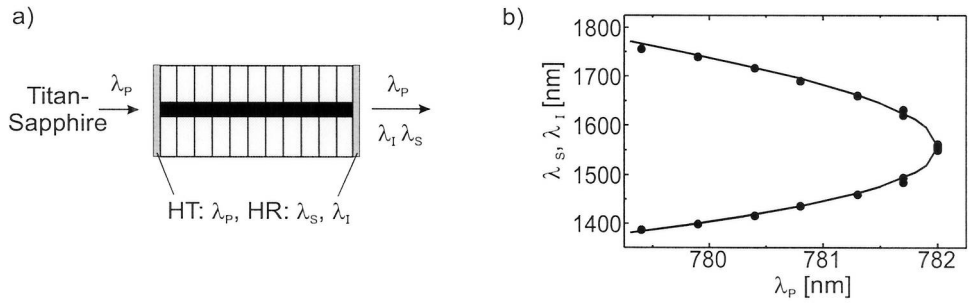

Figure 20. a) Experimental setup and b) tuning characteristic of a NIR DR-IOPO.

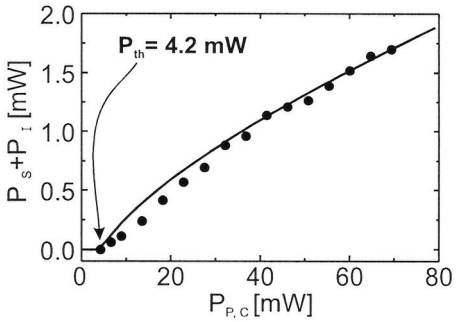

Figure 21. Power characteristic of a NIR DR-IOPO.

6.2. MIR Optical Parametric Oscillators

6.2.1. Doubly Resonant Device

Mid-infrared doubly resonant integrated optical parametric oscillators (DR-IOPOs) in $LiNbO_3$ have been identified as most attractive tunable nonlinear frequency converters with many applications mainly in environmental sensing and process monitoring. Using periodically poled waveguides and exploiting quasi-phase matching low threshold devices can be developed allowing optical pumping with diode lasers.[13] The IOPO consists of a 90 mm long Ti:$LiNbO_3$ waveguide (80 mm periodically poled with periodicity $\sim$31 μm) in a 0.5 mm thick and 12 mm wide Z-cut, X-propagation $LiNbO_3$ substrate with external dielectric mirrors in contact with the waveguide end faces. The periodically poled waveguide has very low losses down to 0.03 dBcm^{-1}. The high quality of the domain grating and excellent homogeneity of the waveguide structure was confirmed by difference-frequency generation yielding a maximum conversion efficiency of 105 %W^{-1} and an effective interaction length of 68 mm. To achieve doubly resonant optical parametric oscillation in the MIR dielectric mirrors are optimized for high signal (λ_s) and idler (λ_i) reflectivity ($>$ 95 %) in the 2800 to 3400 nm spectral range and high pump transmission (80..92 %) between 1500 and 1580 nm. The IOPO is pumped by a tunable, single-frequency external cavity semiconductor laser (1500 nm $< \lambda_P <$ 1580 nm) in combination with a high power (up to 27 dBm) fiber amplifier (see Fig. 22 (left)). The power characteristic of an IOPO with 20 μm wide waveguide is shown in Fig. 22 (right) as signal and idler power versus external pump power. Optical parametric oscillation starts at 14 mW; the corresponding transmitted pump power is only 6.5 mW due to a waveguide coupling efficiency of about 50%. With rising pump power level also signal and idler power increases up to 6.5 mW at 300 mW pump power. At even higher levels the MIR-output saturates at about 7.8 mW. The measured threshold and output characteristic agrees well with modelling results. The tuning behaviour of signal and idler radiation of three IOPOs of different waveguide width has been investigated using a grating monochromator and a Fabry-Perot interferometer (Fig. 23). The maximum continuous tuning range from 2804 to 3379 nm is achieved with the IOPO of 17.5 μm waveguide width and Λ = 31.6 μm domain periodicity by pump wavelength tuning from 1532 to 1570 nm. The overall tuning range is 2765 to 3476 nm determined by the

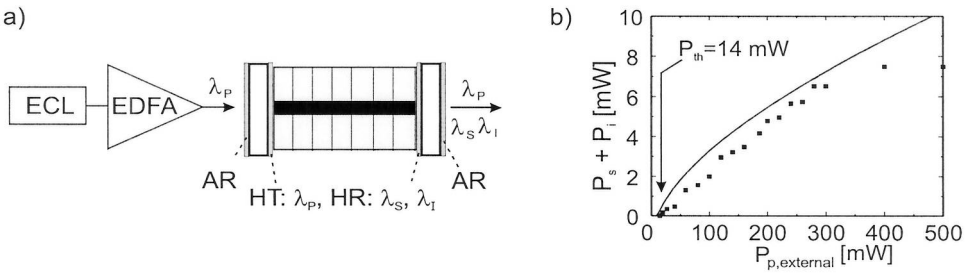

Figure 22. a) Experimental setup and b) power characteristic of a MIR DR-IOPO.

spectral width of the high reflectivity band of the dielectric mirrors. The fine tuning behaviour is determined by the double resonance for signal and idler. As an example, a relative signal frequency is plotted on the right of Fig. 23 as function of the pump frequency detuned from $\lambda_{p0} = 1540$ nm. The signal frequency does not follow the exact phase-matching curve (straight line), but obeys a sawtooth-characteristics with a spectral width of about 180 GHz.

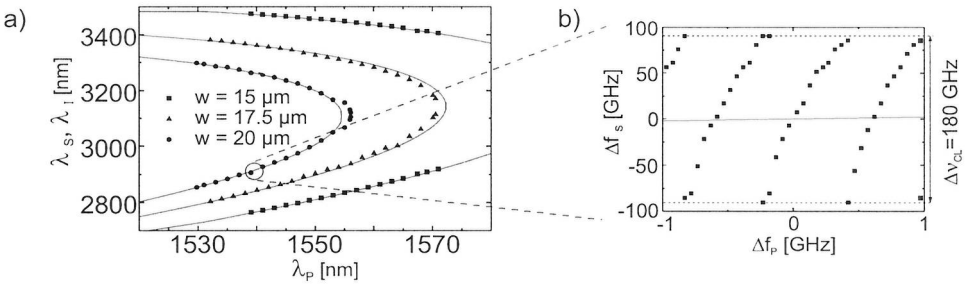

Figure 23. Tuning characteristic of a MIR DR-IOPO.

6.2.2. Singly Resonant Device

Singly resonant integrated optical parametric oscillators (SR-IOPO) are attractive candidates for efficient frequency conversion, nearly continuously tunable in a broad wavelength range without a sawtooth-characteristics as for a doubly-resonant device. Using an annealed proton exchanged waveguide a near-infrared device has been demonstrated with an oscillation threshold of 1.6 W. On the other hand, low-loss Ti:$LiNbO_3$ waveguides allow to reduce the threshold considerably. Our SR-IOPO[14] consists of a 90 mm long channel guide of 17.5 μm width in a Z-cut, X-propagation $LiNbO_3$ substrate. The waveguide losses are as low as 0.06 dB/cm measured at $\lambda = 3391$ nm. Using the electric field poling technique the substrate has been periodically poled over a length of 80 mm with a domain periodicity of 31.3 μm. Dielectric mirrors on a sapphire substrate (R > 95 % for $3200 < \lambda < 3800$ nm, R < 5 % for $2650 < \lambda < 2980$ nm) are in contact with the waveguide end face to form the resonator. A tunable narrow linewidth extended cavity semiconductor laser, amplified by a high power EDFA (33 dBm), is used as pump source to operate and to investigate the SR-IOPO (see Fig. 24). As an example, Fig. 24 (right) presents the power characteristic of the device in cw operation as signal plus idler power in forward direction versus the external pump power ($\lambda_p = 1560$ nm). The oscillation threshold is 275 mW in good agreement with the theoretical prediction, if a 60 % coupling efficiency is assumed. At 1.25 W pump power the mid-infrared emission ($\lambda_s = 2883$ nm, $\lambda_i = 3364$ nm) grows up to ~300 mW; this result corresponds to an overall slope efficiency of 30 %. Due to the SR-configuration of the oscillator the signal power always exceeds the idler power considerably. The SR-IOPO output can be tuned within the range $2720 \text{ nm} < \lambda_s, \lambda_i < 3500$ nm by changing the pump wavelength λ_p from 1530 nm to 1580 nm (see Fig. 25).

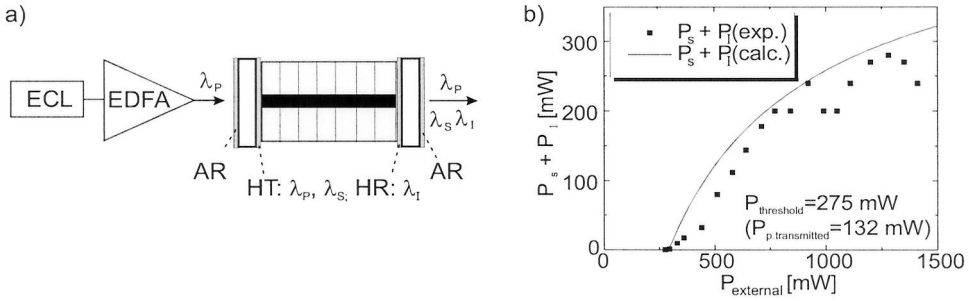

Figure 24. a) Experimental setup and b) power characteristic of a SR-IOPO.

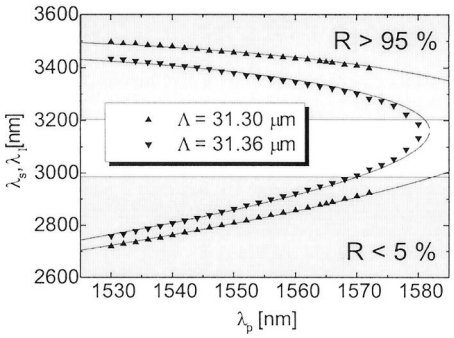

Figure 25. Tuning characteristic of an SR-IOPO.

7. CONCLUSION AND OUTLOOK

Based on our fabrication technology to obtain excellent periodically poled Ti:(Er:)$LiNbO_3$ waveguides we developed a whole family of nonlinear frequency converters of unprecedented efficiency in the near and mid-infrared spectral region:

- NIR second harmonic generation with a normalized efficiency of up to $\eta_{nor} = 935\%\mathrm{W}^{-1}$
- NIR self frequency doubling laser
- NIR difference-frequency generation with $\eta_{nor} = 318\%\mathrm{W}^{-1}$
- cw NIR cascaded difference-frequency generation with $\eta = 25\%$
- pulsed NIR cascaded difference-frequency generation with $\eta = 200\%$ resp. $\eta = 35\%$ at 2 resp. 10 GHz repetition rate
- Cascaded difference frequency generator with up to 4.4 dB gain
- MIR difference frequency generation with $\eta_{nor} = 105\%\mathrm{W}^{-1}$
- NIR and MIR optical parametric fluorescence with several hundred nm tuning range
- Doubly resonant NIR-OPO with 4.2 mW threshold, 350 nm tuning range and 1.7 mW output power
- Doubly resonant MIR-OPO with 14 mW threshold, 400 nm tuning range and 8 mW output power
- Singly resonant MIR-OPO with 275 mW threshold, 600 nm tuning range and 280 mW output power

Our future work will be focused to improve the performance of the frequency converters. This will include:

- exploiting doped $LiNbO_3$ to reduce photorefractive effects
- electrooptic tuning
- development of high performance dielectric mirror coatings on $LiNbO_3$ substrates also for the MIR-range

These improvements will result in very attractive devices for applications in telecommunication and spectroscopy like:

- λ-converters
- ultrabroadband parametric amplifiers
- ultrafast time-division demultiplexers and all optical switches
- mode hop free IOPOs
- synchronously pumped IOPOs to generate tunable short pulses

ACKNOWLEDGMENTS

This work has been supported by the German Ministry of Research and Education under contract 13N7024 and by the ATLAS project founded by the European Union.

REFERENCES

1. M. Flörsheimer, R. Paschotta, U. Kubitschek, Ch. Brillert, D. Hofmann, L. Heuer, G. Schreiber, C. Verbeek, W. Sohler, and H. Fuchs: "Second-harmonic imaging of ferroelectric domains in $LiNbO_3$ with micron resolution in lateral and axial direction", App. Phys. B **67**, 593 (1998).
2. C. Becker, T. Oesselke, J. Pandavenes, R. Ricken, K. Rochhausen, G. Schreiber, W. Sohler, H. Suche, R. Wessel, S. Balsamo, I. Montrosset, and D. Sciancalepore: "Advanced Ti:Er:$LiNbO_3$ waveguide lasers", IEEE J. Sel. Top. Qauntum Electron. **6**, 101 (2000).
3. M. H. Chou, J. Hauden, M. A. Arbore, and M. M. Fejer: "1.5μm-band wavelength conversion based on difference-frequency generation in $LiNbO_3$ waveguides with integrated coupling structures", Opt. Lett. **23**, 1004 (1998).
4. G. Schreiber, R. Ricken and W. Sohler: "Near-infrared second-harmonic and difference-frequency generation in periodically poled Ti:$LiNbO_3$ waveguides", ECIO '99, Torino/Italy, p. 95, April 1999.
5. I. Brener, M. H. Chou, and M. M. Fejer, "Efficient wideband wavelength conversion using cascaded second-order nonlinearities in $LiNbO_3$ waveguides", OFC'99 paper FB6-1.
6. G. Schreiber, D. Hofmann, W. Grundkötter, R. Ricken, and W. Sohler: "Near-infrared cascaded difference-frequency generation in periodically poled Ti:$LiNbO_3$ waveguides", NLGW '99, paper FC3, p. 468, Dijon/France, Sept. 1-3, 1999.
7. K. Gallo, G. Assanto, and G. I. Stegeman, "Efficient wavelength shifting over the erbium amplifier bandwidth via cascaded second order processes in lithium niobate waveguides", Appl. Phys. Lett. **71**, 1020 (1997).
8. D. Hofmann, G. Schreiber, C. Haase, H. Herrmann, R. Ricken, and W. Sohler: "Quasi-phase matched difference-frequency generation in periodically poled Ti:$LiNbO_3$ channel waveguides", Opt. Lett. **24**, 896 (1999).
9. see the review paper: H. Suche and W. Sohler, Optoelectronics-Devices and Technologies, **4**, 1 (1989).
10. M. L. Bortz, M. A. Arbore, and M. M. Fejer: "Quasi-phase matched optical parametric amplification and oscillation in periodically poled $LiNbO_3$ waveguides", Opt. Lett. **20**, 49 (1995).
11. M. A. Arbore and M. M. Fejer: "Singly resonant optical parametric oscillation in periodically poled lithium niobate waveguides", Opt. Lett. **22**, 151 (1997).
12. G. Schreiber, R. Ricken, K. Rochhausen, and W. Sohler: "Doubly resonant near-infrared optical parametric oscillator with periodically poled Ti:$LiNbO_3$ waveguide", CLEO/QELS 2000, paper CThQ2, San Francisco/USA, May 7-12, 2000.

13. D. Hofmann, H. Herrmann, G. Schreiber, W. Grundkötter, R. Ricken, and W. Sohler: "Continuous-wave mid-infrared doubly resonant optical parametric oscillator with periodically poled Ti:$LiNbO_3$ waveguide", OSA Annual Meeting, Santa Clara/USA, paper WP3, Sept. 1999.
14. D. Hofmann, G. Schreiber, W. Grundkötter, R. Ricken, and W. Sohler: "Mid-infrared continuous-wave singly resonant optical parametric oscillator with Periodically Poled Ti:$LiNbO_3$ Waveguide", CLEO/Europe 2000, Nice/France, Sept. 2000.